

Temperature dependence of the energy and broadening parameter of the fundamental band gap of GaSb and $\text{Ga}_{1-x}\text{In}_x\text{As}_y\text{Sb}_{1-y}/\text{GaSb}$ ($0.07 \leq x \leq 0.22$, $0.05 \leq y \leq 0.19$) quaternary alloys using infrared photoreflectance

Martín Muñoz* and Fred H. Pollak†

Physics Department and New York Center for Advanced Technology in Ultrafast Photonic Materials and Applications, Brooklyn College of the City University of New York, Brooklyn, New York 11210

M. B. Zakia and N. B. Patel

LPD/DFA Instituto de Física e Centro de Componentes Semicondutoras, Universidade Estadual de Campinas, Caixa Postal 6165, 13081-970, Campinas, São Paulo, Brazil

J. L. Herrera-Pérez

Centro de Investigación en Ciencia Aplicada y Tecnología Avanzada CICATA-IPN Mexico Distrito Federal, México
(Received 24 May 2000)

We have measured the temperature dependence of the energy [$E_0(T)$] and broadening parameter [$\Gamma_0(T)$] of the fundamental gap for GaSb and four samples of $\text{Ga}_{1-x}\text{In}_x\text{As}_y\text{Sb}_{1-y}$ (lattice matched to GaSb) using infrared photoreflectance. The parameters that describe the temperature variation of the energy (including thermal-expansion effects) were evaluated using both the semiempirical Vashni relation as well as an equation that incorporates the Bose-Einstein occupation factor. The behavior of $\Gamma_0(T)$ was described by a Bose-Einstein-type equation.

I. INTRODUCTION

The quaternary alloy $\text{Ga}_{1-x}\text{In}_x\text{As}_y\text{Sb}_{1-y}$ lattice matched to GaSb is a narrow-band-gap semiconductor ($\sim 0.3\text{--}0.7$ eV at room temperature) with a number of applications including thermophotovoltaic (TPV) cells,¹ infrared light-emitting diodes,² and lasers,^{3–8} as well as photodetectors.^{9,10} The temperature dependence of the fundamental band gap [$E_0(T)$] and the broadening parameter [$\Gamma_0(T)$] are of interest for basic reasons as well as for various applications. The temperature dependence of the energy and linewidth of electronic transitions give important information about the electron-phonon interactions, excitonic effects, etc.^{11,12} From an applied point of view, the ability to measure the band gap at temperatures corresponding to device operating conditions, e.g., 300–350 K for the TPV cells, makes it possible to model certain semiconductor properties at these temperatures. For example, the absorption coefficient of the fundamental gap at these conditions can be evaluated using our previous ellipsometric results on GaSb (Ref. 13) and GaInAsSb (Ref. 14) in conjunction with a comprehensive model for the dielectric function which involves both discrete and continuous excitonic effects at the $E_0/E_0 + \Delta_0$ and $E_1/E_1 + \Delta_1$ critical points.¹⁵

However, in spite of its significance, few works on the temperature dependence of the fundamental band gap of GaSb have been reported and none for these quaternary compounds. An early study of $E_0(T)$ of GaSb was done by Joullié *et al.*¹⁶ using Schottky barrier electroreflectance between 30 and 300 K. However, the data were fit using only a linear term which produced an overestimation of the value of $E_0(0)$, which is frequently quoted in the literature.¹⁷ There are reports of the temperature dependence of the higher lying

transition $E_0 + \Delta_0$ between 4 and 300 K (Ref. 18) and $E_0 + \Delta_0$, $E_1, E_1 + \Delta_1$ between 83 and 300 K.¹⁹

In this work we present the temperature dependence of $E_0(T)$ and the related broadening parameter [$\Gamma_0(T)$] for GaSb and four $\text{Ga}_{1-x}\text{In}_x\text{As}_y\text{Sb}_{1-y}/\text{GaSb}$ (001) ($0.07 \leq x \leq 0.22$, $0.05 \leq y \leq 0.19$) quaternary alloys, using infrared-photoreflectance (IRPR) between 15 and 377 K. The four quaternary samples have compositions of ($x=0.07$, $y=0.05$), ($x=0.09$, $y=0.07$), ($x=0.12$, $y=0.11$), and ($x=0.22$, $y=0.19$). The band gap of the quaternaries decreases with increasing In composition. In narrow-band-gap materials the applications of photoreflectance (PR) have been limited by the low values of the built-in field. However, to our knowledge there has been no study of the PR applicability limits to these narrow-band-gap materials. During this study we were able to test the usefulness of PR for these materials. The temperature dependence of band gaps has been described by equations involving three parameters, such as the Varshni expression²⁰ or one containing the Bose-Einstein occupation factor for phonons and involving the electron-average phonon (acoustical and optical) interaction.^{11,12} By taking into account the component of the energy gap shift due to the thermal-expansion coefficient, we have obtained revised parameters which are directly related to the electron-average phonon interaction in the latter case. A somewhat similar Bose-Einstein-type equation, involving the electron-longitudinal optical (LO) phonon at $\mathbf{q} \approx 0$ (Fröhlich interaction), has been used to fit the temperatures dependence of the broadening function.^{11,12}

II. EXPERIMENTAL DETAILS

The GaSb and the $\text{Ga}_{1-x}\text{In}_x\text{As}_y\text{Sb}_{1-y}$ epitaxial layers, lattice matched to GaSb (001) substrates, were grown by liquid

TABLE I. Carrier concentration and type as well as lattice-mismatch data of the studied samples.

Sample	Carrier concentration/type (10^{16} cm^{-3})	$\Delta a/a$ (10^{-4})
GaSb	$17/n^a$	0
$\text{Ga}_{0.93}\text{In}_{0.07}\text{As}_{0.05}\text{Sb}_{0.95}$	$6/p^b$	0
$\text{Ga}_{0.91}\text{In}_{0.09}\text{As}_{0.07}\text{Sb}_{0.93}$	$5/p^b$	5.1
$\text{Ga}_{0.88}\text{In}_{0.12}\text{As}_{0.11}\text{Sb}_{0.89}$	$4/n^a$	2
$\text{Ga}_{0.78}\text{In}_{0.22}\text{As}_{0.19}\text{Sb}_{0.81}$	$2/p^b$	-3.5

^aTe doped.

^bNominally undoped.

phase epitaxy (LPE) in a graphite sliding boat using a Pd-diffused hydrogen atmosphere. The starting materials were (6N)Ga, In, Sb, and undoped GaAs. The growth temperatures were in the range of 520–530 °C except for the layer with the highest In solid composition, which was grown at 605 °C. This composition is at the edge of the miscibility gap, which is around of $x=0.23$ for the (001) orientation.²¹ The solid composition was determined by electron microprobe analysis and the lattice mismatch evaluated by double crystal x-ray-diffraction measurements. The nominally undoped layers are p type while the n -type layers are Te doped. The Hall measurements for the p -type films were performed at 77 K because the substrates have semi-insulating characteristics only up to 150 K so that, at higher temperatures part of the current is conducted by the substrate producing a non-reliable carrier measurements. For the n -type films the existence of a p - n junction provides reliable measurements even at room temperature. The GaSb substrates employed have a net carrier concentration equal to $2 \times 10^{14} \text{ cm}^{-3}$ at 77 K. The carrier concentration and type as well as the lattice-mismatch are summarized in Table I.

The basic PR experimental setup is described elsewhere.²² Prior PR investigations have been reported to only about 0.7 eV.²² To extend the range of our measurements we employed a monochromator with a 300-line/mm diffraction grating (blazed at $2 \mu\text{m}$), a 170 W tungsten-halogen lamp, a thermoelectrically cooled InAs detector operated at -30 C , and silica lenses. He-Ne lasers ($\lambda = 632.8 \text{ nm}$) with intensities of 5 and 10 mW were used for temperatures below and above 150 K, respectively.

III. EXPERIMENTAL RESULTS AND ANALYSIS

The solid lines in Figs. 1(a)–1(c), are the experimental IRPR spectra for GaSb, and quaternary samples $\text{Ga}_{0.88}\text{In}_{0.12}\text{As}_{0.11}\text{Sb}_{0.89}$ and $\text{Ga}_{0.78}\text{In}_{0.22}\text{As}_{0.19}\text{Sb}_{0.81}$, respectively, at three different temperatures. The curves for different temperatures have been displaced for clarity. The dashed lines are least-squares fits to a line shape which contains Lorentzian broadened electro-optic functions,²² yielding the values of $E_0(T)$, designated by the arrows, as well as $\Gamma_0(T)$.

Displayed by the solid squares in Fig. 2 are the obtained values of $E_0(T)$ for GaSb and all the quaternary samples. Representative error bars are shown. The quantity $E_0(T)$ was fit using both the Varshni²⁰ and Bose-Einstein-type^{11,12} expressions.

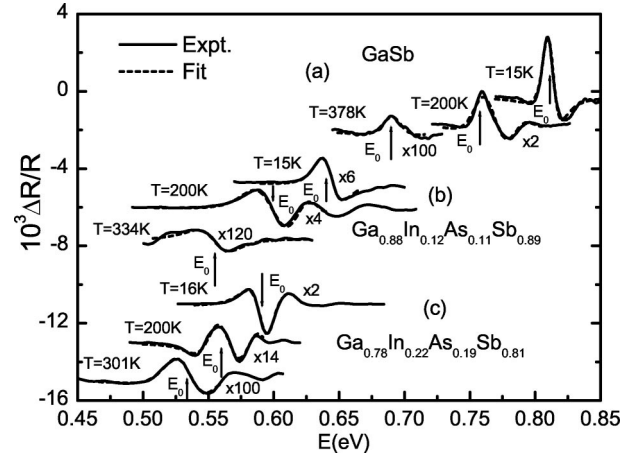


FIG. 1. The solid lines are the IRPR spectra for samples (a) GaSb, (b) $\text{Ga}_{0.88}\text{In}_{0.12}\text{As}_{0.11}\text{Sb}_{0.89}$, and (c) $\text{Ga}_{0.78}\text{In}_{0.22}\text{As}_{0.19}\text{Sb}_{0.81}$ at three different temperatures. The dashed lines are the least-squares fits to a line-shape function yielding the $E_0(T)$ values indicated by arrows. The curves have been displaced for clarity.

The Varshni equation is given by²⁰

$$E_0(T) = E_0(0) - \frac{\alpha T^2}{\beta + T}, \quad (1)$$

where $E_0(0)$ is the band gap at $T=0 \text{ K}$ while α and β are the so-called Varshni coefficients. The Bose-Einstein-type expression, which involves electron coupling to an average phonon (optical and acoustical), is given by^{11,12}

$$E_0(T) = E_0(0) - \frac{2a_B}{\exp(\Theta_B/T) - 1}, \quad (2)$$

where a_B is the strength of the electron-average phonon interaction and Θ_B is the average phonon temperature.

The dashed and solid lines in Fig. 2 are least-squares fits to Eqs. (1) and (2), respectively. Listed in Table II are the obtained values of $E_0(0)$, α , β , a_B and Θ_B for the five samples.

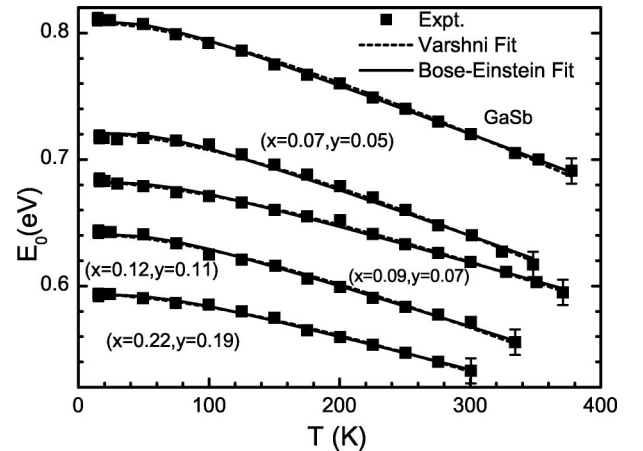


FIG. 2. The solid squares are the experimental values of $E_0(T)$ for the different samples. The (x, y) notation represents the composition of the quaternary samples. Representative bars are shown. The dashed and continuous lines are the fits according to the Varshni relation [Eq. (1)] and the Bose-Einstein [Eq. (2)] expressions, respectively.

TABLE II. Values of the Varshni [Eq. (1)] and Bose-Einstein-type [Eq. (2)] fit parameters for GaSb and the four quaternary samples.

Sample	Varshni fit			Bose-Einstein-type fit		
	$E_0(0)$ (eV)	α (10^{-4} eV/K)	β (K)	$E_0(0)$ (eV)	a_B (meV)	Θ_B (K)
GaSb	0.809 ± 0.005	5.3 ± 0.4	234 ± 40	0.809 ± 0.005	35 ± 5	175 ± 30
$\text{Ga}_{0.93}\text{In}_{0.07}\text{As}_{0.05}\text{Sb}_{0.95}$	0.721 ± 0.005	5.2 ± 0.4	274 ± 40	0.721 ± 0.005	38 ± 5	198 ± 30
$\text{Ga}_{0.91}\text{In}_{0.09}\text{As}_{0.07}\text{Sb}_{0.93}$	0.683 ± 0.005	3.9 ± 0.4	250 ± 40	0.682 ± 0.005	27 ± 5	186 ± 30
$\text{Ga}_{0.88}\text{In}_{0.12}\text{As}_{0.11}\text{Sb}_{0.89}$	0.641 ± 0.005	4.7 ± 0.4	271 ± 40	0.641 ± 0.005	32 ± 5	188 ± 30
$\text{Ga}_{0.78}\text{In}_{0.22}\text{As}_{0.19}\text{Sb}_{0.81}$	0.594 ± 0.005	4.0 ± 0.4	290 ± 40	0.593 ± 0.005	26 ± 5	191 ± 30

The temperature shift of $E_0(T)$ contains contributions from both thermal-expansion and electron-average phonon effects. Therefore, in order to obtain parameters directly related to the latter interaction, it is necessary to eliminate the effects of the former. The energy shift ΔE_{th} due to the thermal expansion can be written as²³

$$\Delta E_{\text{th}} = -3a_H \int_0^T \alpha_{\text{th}}(T) dT, \quad (3)$$

where a_H is the hydrostatic deformation potential and $\alpha_{\text{th}}(T)$ is the linear-expansion coefficient. In order to remove the thermal-expansion contribution to $E_0(T)$ we rewrite Eqs. (1) and (2) as²⁴

$$E_0(T) - \Delta E_{\text{th}} = E_0'(0) - \frac{\alpha' T^2}{\beta' + T}, \quad (4)$$

$$E_0(T) - \Delta E_{\text{th}} = E_0'(0) - \frac{2a'_B}{\exp(\Theta'_B/T) - 1}, \quad (5)$$

respectively.

While $\alpha_{\text{th}}(T)$ and the hydrostatic deformation potential (a) for GaSb are known, in order to evaluate these quantities for the quaternary compounds we used an interpolation scheme based on the four binaries:

$$Q_{\text{quat}}(x, y) = xyQ_{\text{InAs}} + x(1-y)Q_{\text{InSb}} + y(1-x)Q_{\text{GaAs}} + (1-x)(1-y)Q_{\text{GaSb}}, \quad (6)$$

where $Q_i = \alpha_{\text{th},i}$ or a_i ($i = \text{quat}, \text{InAs}, \text{etc.}$). The data for the binary compounds were taken from Refs. 25 and 26.

The solid and open symbols in Fig. 3 are $E_0(T)$ and $E_0(T) - \Delta E_{\text{th}}(T)$, respectively, for the GaSb and $\text{Ga}_{0.78}\text{In}_{0.22}\text{As}_{0.19}\text{Sb}_{0.81}$ samples. For clarity we show only these two materials. The dashed and solid lines represent least-squares fits to Eqs. (2) and (5), respectively. The data have also been fit using Eq. (4). The obtained values for $E_0'(0)$, a'_B , Θ'_B , α' , and β' are presented in the Table III.

The temperature dependence of the linewidth [full width at half maximum (FWHM)], can be expressed as^{11,12}

$$\Gamma_0(T) = \Gamma_0(0) + \frac{\Gamma_{\text{LO}}}{\exp(\Theta_{\text{LO}}/T) - 1}, \quad (7)$$

where $\Gamma_0(0)$ is the broadening mechanism due to intrinsic lifetime, electron-electron interaction, impurity, dislocation,

and alloy scattering effects, Γ_{LO} is the electron-LO phonon coupling constant (Fröhlich interaction) and Θ_{LO} is the LO phonon temperature.

In Fig. 4 the closed squares are the experimental values of $\Gamma_0(T)$ for the GaSb and $\text{Ga}_{0.78}\text{In}_{0.22}\text{As}_{0.19}\text{Sb}_{0.81}$ samples, respectively. For clarity the corresponding data for the other samples are not shown. Because of the error bars on our data it was necessary to fix the parameter Θ_{LO} in order to obtain the two significant quantities $\Gamma_0(0)$ and Γ_{LO} by means of a least-squares fit of Eq. (7). The estimation of Θ_{LO} for the quaternary samples has been done using the interpolation scheme given by Eq. (6), the corresponding binary values were obtained from Ref. 25. The solid lines in Fig. 4 are least-squares fits to Eq. (7). Listed in Table IV are the obtained values of $\Gamma_0(0)$ and Γ_{LO} as well as Θ_{LO} (fixed).

IV. DISCUSSION OF RESULTS

Mannogian and Woolley²⁷ have suggested that after the thermal-expansion term is removed the parameter β' of Eq. (4) is related to the Debye temperature (Θ_D) by $\beta' = 3/8\Theta_D$. Listed in Table III are $\frac{3}{8}\Theta_D$ for GaSb and the four quaternaries, the latter Θ_D being evaluated using Eq. (6) and the binary values from Refs. 25 and 26. There is good agreement between the values of β' and $\frac{3}{8}\Theta_D$.

From the high-temperature limit of Eqs. (4) and (5) the parameters α' , a'_B , and Θ'_B are related by $\alpha' = 2a'_B/\Theta'_B$.

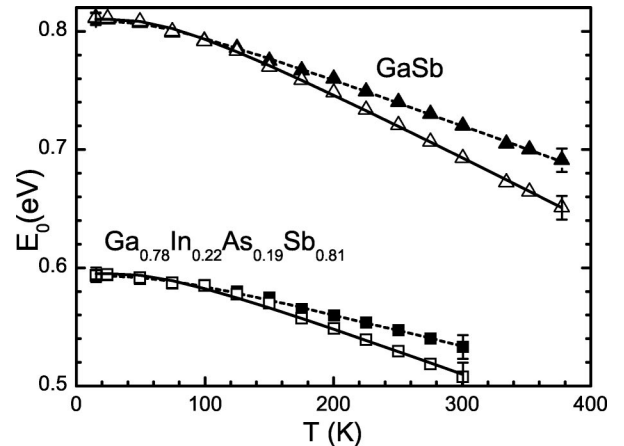


FIG. 3. The solid and open symbols represent $E_0(T)$ values with and without the thermal-expansion contribution, respectively. Representative bars are shown. The dashed and continuous lines represent the fits according to Eqs. (2) and (5), respectively.

TABLE III. Values of the Varshni [Eq. (4)] and Bose-Einstein-type [Eq. (5)] fit parameters (after removal of ΔE_{th}) for GaSb and the four quaternary samples. Also listed are $\frac{3}{8}\Theta_D$ and $2a'_B/\Theta'_B$.

Sample	Varshni fit			Bose-Einstein-type fit				
	$E'_0(0)$ (eV)	α' (10^{-4} eV/K)	β' (K)	$\frac{3}{8}\Theta_D$ (K)	$E'_0(0)$ (eV)	a'_B (meV)	Θ'_B (K)	$2a'_B/\Theta'_B$ (10^{-4} eV/K)
GaSb	0.812 ± 0.005	5.4 ± 0.4	113 ± 40	100	0.809 ± 0.005	62 ± 5	217 ± 30	5.7
$\text{Ga}_{0.93}\text{In}_{0.07}\text{As}_{0.05}\text{Sb}_{0.95}$	0.723 ± 0.005	5.1 ± 0.4	130 ± 40	100	0.722 ± 0.005	49 ± 5	194 ± 30	5.1
$\text{Ga}_{0.91}\text{In}_{0.09}\text{As}_{0.07}\text{Sb}_{0.93}$	0.684 ± 0.005	4.2 ± 0.4	122 ± 40	100	0.683 ± 0.005	48 ± 5	215 ± 30	4.5
$\text{Ga}_{0.88}\text{In}_{0.12}\text{As}_{0.11}\text{Sb}_{0.89}$	0.645 ± 0.005	4.7 ± 0.4	122 ± 40	100	0.643 ± 0.005	46 ± 5	196 ± 30	4.7
$\text{Ga}_{0.78}\text{In}_{0.22}\text{As}_{0.19}\text{Sb}_{0.81}$	0.595 ± 0.005	3.9 ± 0.4	130 ± 40	100	0.594 ± 0.005	39 ± 5	200 ± 30	3.9

Table III shows that this relationship is indeed satisfied. The results in Fig. 3 show that the thermal-expansion effect is responsible for only about 4% of the total band-gap variation at room temperature.

The analysis of Joullié *et al.*¹⁶ for $E_0(T)$ of GaSb consisted of only a linear fit between 100 and 300 K with a slope of -3.5×10^{-4} eV/K. Using this value and $E_0(300 \text{ K}) = 0.72$ eV,^{17,19} the extrapolated number is $E_0(0) = 0.825$ eV, which is the value frequently quoted in the literature.¹⁷ However, $E_0(T)$ for direct gap semiconductors at low temperatures differs considerably from a straight line^{11,12} and hence $E_0(0)$ has been overestimated by Ref. 16. Our value for this parameter, using both the Varshni and the Bose-Einstein-type equations, is $E_0(0) = 0.809$ eV, which is in agreement with the value of 0.8099 eV obtained from photoluminescence measurements at 2 K.²⁸

The value of α [$(5.26 \pm 0.4) \times 10^{-4}$ eV/K] for E_0 in GaSb reported in this work is in good agreement with those presented by Hwang *et al.*¹⁹ ($\alpha = 6.5 \times 10^{-4}$ eV/K) and Iyer *et al.*¹⁸ ($\alpha = 5.5 \times 10^{-4}$ eV/K) for the $E_0 + \Delta_0$ transition. While our number for β [(234 ± 40) K] is similar to Hwang *et al.* (230 K) it is somewhat higher than that of Ref. 18 (175 K).

Our values for Γ_{LO} are considerable smaller than those reported previously for a number of III-V (GaAs, InGaAs) and II-VI [ZnSe, CdSe (cubic), ZnCdSe] zinc-blende-type semiconductors, except for two measurements of Γ_{LO}

$= 7-8$ meV for GaAs.^{22,24} This difference may be due to the relatively weak Fröhlich coupling constant C_F in our samples in relation to the other reported zinc-blende materials, where²⁹

$$C_F \propto \left[\Theta_{\text{LO}} \left(\frac{1}{\varepsilon_\infty} - \frac{1}{\varepsilon_0} \right) \right]^{1/2}. \quad (8)$$

In this equation ε_∞ and ε_0 are the high-frequency and the static dielectric constants, respectively. For example, using the data of Ref. 26 we obtained $C_F(\text{GaSb})/C_F(\text{GaAs}) = 0.56$ and $C_F(\text{GaSb})/C_F(\text{ZnSe}) = 0.30$.

The band-gap values at room temperature of our samples agree with those presented in Table I by DeWinter *et al.*³⁰ However, neither the relations for the band gap as function of the composition presented by these authors nor the one presented by Wang *et al.*³¹ provide a good description of E_0 for indium compositions higher than 10%. The use of any of these relations to determine the composition of rich indium films can produce compositions errors up to 5%, including one of our previous reports.¹⁴

IV. SUMMARY

In this work we have presented the temperature dependence of the fundamental band gap and broadening parameter of GaSb and four $\text{Ga}_{1-x}\text{In}_x\text{As}_y\text{Sb}_{1-y}$ alloys between 14 and 377 K. We have described $E_0(T)$ in terms of both the Varshni and Bose-Einstein-type equations. As a consequence of this analysis we obtained the correct value for $E_0(0) = 0.809$ eV for GaSb and the corresponding ones for the quaternaries compounds. In addition, we have separated the thermal-expansion and electron-average phonon contributions to $E_0(T)$ and concluded that the former is responsible

TABLE IV. Values of the Bose-Einstein-type [Eq. (7)] fit parameters for GaSb and the four quaternary samples.

Sample	Γ_0 (meV)	Γ_{LO} (meV)	Θ_{LO} (K)
GaSb	10.4 ± 0.5	7 ± 3	335 ^a
$\text{Ga}_{0.93}\text{In}_{0.07}\text{As}_{0.05}\text{Sb}_{0.95}$	12.2 ± 0.5	7 ± 3	332.9 ^a
$\text{Ga}_{0.91}\text{In}_{0.09}\text{As}_{0.07}\text{Sb}_{0.93}$	11.8 ± 0.5	9 ± 3	332.9 ^a
$\text{Ga}_{0.88}\text{In}_{0.12}\text{As}_{0.11}\text{Sb}_{0.89}$	16.3 ± 0.5	8 ± 3	333.6 ^a
$\text{Ga}_{0.78}\text{In}_{0.22}\text{As}_{0.19}\text{Sb}_{0.81}$	12.9 ± 0.5	8 ± 3	331.7 ^a

^aParameter fixed.

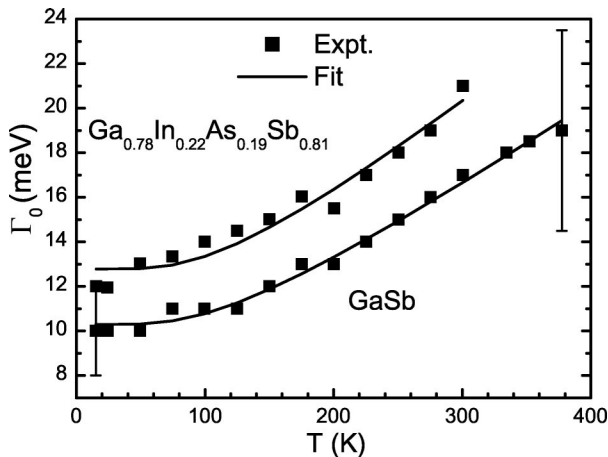


FIG. 4. The solid squares are $\Gamma_0(T)$ for the GaSb and $\text{Ga}_{0.78}\text{In}_{0.22}\text{As}_{0.19}\text{Sb}_{0.81}$ samples. The solid lines are the fit according to the Bose-Einstein relation [Eq. (7)]. Representative bars are shown.

for only 4% of the shift at room temperature. The temperature dependence of the linewidth was described using a Bose-Einstein equation. The small value of Γ_{LO} may be related to the relatively weak Fröhlich interaction in our materials in relation to other zinc-blende-type semiconductors.

We have implemented an IRPR system with capabilities at long wavelengths and utilized it to determine $E_0(T)$ and $\Gamma_0(T)$ for narrow band-gap materials.

ACKNOWLEDGMENTS

Two of the authors (M.M. and F.H.P.) thank to the New York State Science and Technology Foundation through its Centers for Advanced Technology program for support of this project. Also M.M. acknowledges support from CONA-CyT, Mexican Agency, through Research Project No. 25135E.

*Permanent address: Departamento de Física CINVESTAV-IPN, México D.F., México, 07300. Electronic address: martin@fis.cinvestav.mx

[†]Also at the Graduate School and University Center of the City University of New York, New York, NY 10016. Electronic address: fhpbc@cunyvm.cuny.edu

¹G. W. Charache, J. L. Egle, D. M. Depoy, L. R. Danielson, M. J. Freeman, R. J. Dziendziel, J. F. Moynihan, P. F. Baldasaro, B. C. Campbell, C. A. Wang, H. K. Choi, G. W. Turner, S. J. Wojtczuk, P. Colter, P. Sharps, M. Timmons, R. E. Fahey, and K. Zhang, *J. Electron. Mater.* **27**, 1038 (1998).

²A. Andaspaeva, A. N. Baranov, and A. Gusseinov, *Pis'ma Zh. Tekh. Fiz.* **14**, 845 (1988) [*Sov. Tech. Phys. Lett.* **14**, 377 (1988)].

³C. Caneau, A. K. Srivastava, A. G. Dentai, J. L. Zyskind, and M. A. Pollack, *Electron. Lett.* **21**, 815 (1985).

⁴A. E. Drakin, P. G. Eliseev, B. N. Sverdlov, A. E. Bochkarev, L. M. Dolginov, and L. V. Druzhinia, *IEEE J. Quantum Electron.* **23**, 1089 (1987).

⁵C. A. Wang and H. K. Choi, *J. Electron. Mater.* **26**, 1231 (1997); *Appl. Phys. Lett.* **70**, 802 (1997).

⁶M. B. Z. Morosini, J. L. Herrera-Pérez, M. S. S. Loral, A. A. G. Von Zuben, A. C. F. de Silveira, and N. B. Patel, *IEEE J. Quantum Electron.* **QE-29**, 2103 (1993).

⁷H. K. Choi, J. N. Walpole, G. W. Turner, M. K. Connors, L. J. Missaggia, and M. J. Manfra, *IEEE Photonics Technol. Lett.* **10**, 938 (1998).

⁸M. F. Flatte, C. H. Grein, H. Ehrenreich, R. H. Miles, and H. Cruz, *J. Appl. Phys.* **78**, 4552 (1995).

⁹Y. Shi, J. H. Zhao, J. Sarathy, H. Lee, and G. H. Olsen, *IEEE Trans. Electron Devices* **44**, 2167 (1997).

¹⁰K. Xie, J. H. Zhao, Y. Shi, H. Lee, and G. H. Olsen, *IEEE Photonics Technol. Lett.* **8**, 667 (1996).

¹¹P. Lautenschlager, M. Garriga, and M. Cardona, *Phys. Rev. B* **35**, 9174 (1987).

¹²P. Lautenschlager, P. B. Allen, and M. Cardona, *Phys. Rev. B* **33**, 5501 (1986).

¹³M. Muñoz, K. Wei, F. H. Pollak, J. L. Freeouf, and G. W. Charache, *Phys. Rev. B* **60**, 8105 (1999).

¹⁴M. Muñoz, K. Wei, F. H. Pollak, J. L. Freeouf, C. A. Wang, and G. W. Charache, *J. Appl. Phys.* **87**, 1780 (2000).

¹⁵T. Holden, P. Ram, F. H. Pollak, J. L. Freeouf, B. X. Yang, and M. C. Tamargo, *Phys. Rev. B* **56**, 4037 (1997).

¹⁶A. Joullié, A. Zein Eddin, and B. Girault, *Phys. Rev. B* **23**, 928 (1981).

¹⁷P. S. Dutta and H. L. Bhat, *J. Appl. Phys.* **82**, 5821 (1997).

¹⁸S. Iyer, S. Mulugeta, W. Collis, S. Venkatraman, K. K. Bajaj, and G. Coli, *J. Appl. Phys.* **87**, 2336 (2000).

¹⁹J. S. Hwang, S. L. Tyan, and Y. K. Su, *Solid State Commun.* **80**, 891 (1991).

²⁰K. P. Varshni, *Physica (Utrecht)* **34**, 149 (1967).

²¹J. L. Lazzari, E. Tournié, F. Pitard, and A. Joullié, *Mater. Sci. Eng.*, **B 9**, 125 (1991).

²²F. H. Pollak, in *Handbook on Semiconductors*, edited by M. Balkanski (North-Holland, New York, 1993), Vol. 2.

²³P. Lautenschlager, P. B. Allen, and M. Cardona, *Phys. Rev. B* **31**, 2163 (1985).

²⁴L. Malikova, W. Krystek, F. H. Pollak, N. Dai, A. Cavus, and M. C. Tamargo, *Phys. Rev. B* **54**, 1819 (1996).

²⁵*Numerical Data and Functional Relationships in Science and Technology*, edited by O. Madelung, M. Schultz, and H. Weiss, Landolt-Börnstein, Group III, Vol. 17a (Springer, New York, 1982).

²⁶*Semiconductors-Basic Data*, 2nd edition, edited by O. Madelung (Springer, Berlin, 1996).

²⁷A. Manoogian and J. C. Woolley, *Can. J. Phys.* **62**, 285 (1984).

²⁸M. Rühle, R. L. Aggarwal, and B. Lax, *Phys. Rev. B* **5**, 3033 (1972).

²⁹P. Y. Yu and M. Cardona, *Fundamentals of Semiconductors: Physics and Materials Properties* (Springer, Berlin, 1996).

³⁰J. C. DeWinter, M. A. Pollack, A. K. Srivastava, and J. L. Zyskind, *J. Electron. Mater.* **14**, 729 (1985).

³¹C. A. Wang, H. K. Choi, D. C. Oakley, and G. W. Charache, *J. Cryst. Growth* **195**, 346 (1998).